Available online at www.sciencedirect.com
SCIENCE DIRECT®
Physica B 365 (2005) 141–146
PHYSICA B
www.elsevier.com/locate/physb

The magneto-transport properties of epitaxial $La_{0.7}Sn_{0.3}MnO_3$ manganite thin films

T.Y. Cheng[a,*], C.C. Hsieh[a], J.Y. Juang[a], J.-Y. Lin[b], K.H. Wu[a], T.M. Uen[a], Y.S. Gou[a], C.H. Hsu[c]

[a]*Department of Electrophysics, National Chiao Tung University, Hsinchu, Taiwan*
[b]*Institute of Physics, National Chiao Tung University, Hsinchu, Taiwan*
[c]*National Synchrotron Radiation Research Center, Hsinchu, Taiwan*

Received 20 March 2005; received in revised form 27 April 2005; accepted 8 May 2005

Abstract

Single-phase $La_{0.7}Sn_{0.3}MnO_3$ (LSnMO) thin films were fabricated on $SrTiO_3$ (STO) substrates by pulsed laser deposition (PLD). The as-deposited films, though were insulating with no sign of insulator-–metal transition (IMT), did display paramagnetic–ferromagnetic transition (PFT) around 150 K. Ex situ annealing of the films at 850 °C in 250 Torr oxygen for 4 h, nonetheless, not only significantly improves the crystallographic quality but also raises IMT and PFT at 315 K and 320 K, respectively. The manifestations of spin-glass-like behavior in both the as-deposited and post-annealed films suggest that it could be intrinsic LSnMO, albeit transport properties can be drastically changed by the strain originating from large ion-size misfit between Sn and La and film/substrate epitaxial relation. The preliminary X-ray absorption spectroscopy shows signature of Mn^{3+}/Mn^{2+} mixed-valence indicating that tetravalent Sn ions does result in electron-doping into the e_g band of Mn.
© 2005 Elsevier B.V. All rights reserved.

PACS: 81.40.Rs; 75.30.Vn; 75.50.Lk

Keywords: Strain relaxation; Spin glass; Magnetoresistance

1. Introduction

The colossal magnetoresistance (CMR) effect and associated exotic physical properties exhibited in various hole-doped perovskite manganites have been subject of extensive researches [1,2]. On the other hand, due to the large size differences between the trivalent La^{3+} and tetravalent ions, it is generally very difficult to obtain single-phase electron-doped manganites by ionic substitution. In fact, Joseph Joly et al. [3] even argued that it is almost impossible to replace La^{3+} by tetravalent

*Corresponding author. Tel.: +88635731943; fax: +88635725230.
E-mail address: melin.ep89g@nctu.edu.tw (T.Y. Cheng).

0921-4526/$ - see front matter © 2005 Elsevier B.V. All rights reserved.
doi:10.1016/j.physb.2005.05.007

ions in polycrystalline manganite bulks. Indeed, all early attempts in preparing Ce-doped $RMnO_3$ (R = La, Pr, Nd) manganites by Das and Mandal [4] showed signatures of mixed-phases and hence blurred the interpretation of the obtained results. In particular, it has been argued [5,6] that the replacement of tetravalent ions to La^{3+} could lead to the self-doped $La_{1-x}MnO_{3-\delta}$ with localized multiphase compounds, which might give rise to very similar magneto-transport properties to those of the hole-doped manganites and jeopardize the genuine characteristics of electron doping.

Recently, successful fabrication of single-phase electron-doped $La_{0.7}Ce_{0.3}MnO_3$ (LCeMO) thin films by pulsed laser deposition (PLD) has been demonstrated [7–9], indicating that ionic constraints and stoichiometry conservation can both be compromised provided proper growth conditions were chosen [8]. Compared to LCeMO, obtaining single-phase $La_xSn_{1-x}MnO_3$ encounters an even more severe challenge because of the larger ionic-size misfit between La^{3+} and Sn^{4+}. Nevertheless, CMR effect has been reported in several $La_xSn_{1-x}MnO_3$ and Fe-doped $La_xSn_{1-x}MnO_3$ systems [10–12], albeit the phases formed were still a matter of discussion [13] and only limited doping ($x = 0.04-0.2$) has been achieved in the thin film form [11,12]. Since most manganites display optimum CMR effects at $x \approx 0.3$, it is desirable to extend the study of $La_xSn_{1-x}MnO_3$ to higher doping. In this paper, we report results of fabricating perovskite-like single-phase $La_{0.7}Sn_{0.3}MnO_3$ (LSnMO) films epitaxially grown on $SrTiO_3$ (STO) substrates by PLD. Although, the as-deposited (AD) films were insulating, it was found that ex situ post-deposition annealing not only raises the paramagnetic–ferromagnetic (PM–FM) transition temperature T_c from 175 to over 320 K but also drives the films to display a typical insulator-–metallic transition at $T_{IM} \approx 315$ K. The significant spin-glass-like behavior [14] observed in both AD and annealed films indicates that the absence of insulator–metal transition in the AD film is not due to spin-glass-induced effects [15]. Preliminary X-ray absorption spectroscopy (XAS) also indicates the presence of Mn^{2+}/Mn^{3+} signature, indicating the realization of electron doping by Sn substitution.

2. Experimental

Sintered LSnMO target was prepared by conventional solid-state reaction technique. Briefly, La_2O_3 and SnO_2 powder were first calcined at 800 °C for 8 h. The calcined product was then mixed and ground with stoichiometric (with nominal $x = 0.3$) amount of $MnCO_3$ and sintered at 1200 °C for 30 h. After repeating the grind-and-sinter process three times, it was pressed into a pellet and sintered at 1200 °C for 72 h. LSnMO films with a typical thickness of about 200 nm were deposited on single-crystalline STO(1 0 0) substrates using a 248 nm KrF excimer laser operating at energy density of 2–3 J/cm^2 and repetition rate of 5–10 Hz. In trying to obtain LSnMO films displaying CMR behavior in situ, we had changed the substrate temperature (T_s) from 25 to 800 °C while keeping the oxygen partial pressure (PO_2) at 0.35 Torr. However, all the AD films, though exhibited PM–FM transition at lower temperatures, were insulating and did not show metallic transition. Consequently, post-deposition ex situ anneals were carried out at 850 and 800 °C, respectively, in 250 Torr oxygen for 4 h for films obtained at each T_s. Since the results are rather extensive, otherwise specified, we will compare mostly the results of two representative samples here and leave the systematic comparisons to a separate publication. The temperature dependences of magnetization ($M(T)$) and magneto-transport properties were measured using a Quantum Design® PPMS system with a maximum applied field strength of 8 T.

3. Results and discussion

Fig. 1(a) compares the X-ray diffraction (XRD) results for an AD film obtained at $T_s = 780$ °C to that of a film deposited at the same T_s but ex situ post-annealed (referred as PA hereafter) at 850 °C. As is evident from the results, both the AD and PA films have no observable impurity phases. The energy dispersive spectroscopy analysis for both films shows an average composition ratio of La:Sn:Mn = 0.756:0.295:1 (normalized to Mn = 1), in good agreement with the nominal

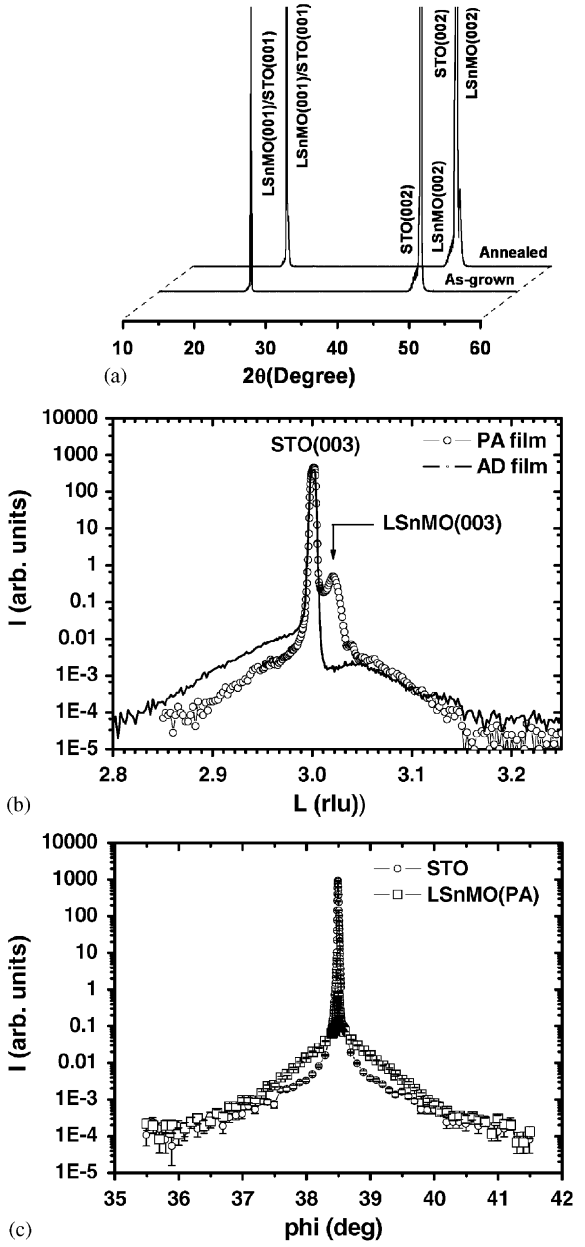

Fig. 1. (a) XRD results for the as-deposited (AD) and post-annealed (PA) LSnMO films grown on STO substrate at $T_s = 780\,^{\circ}C$. (b) L-scan of AD and PA films across (0 0 3) Bragg peak. (c) The Phi (azimuthal) scan across the STO (2 2 2) and LSMO (2 2 2) Bragg peaks, respectively.

stoichiometry of the target. For further clarification, L scan of AD and PA films across (0 0 3) Bragg peak were performed, as displayed in Fig. 1(b). We note that a similar peak alignment was obtained for the AD film, except that the peak width of the film is wider, presumably due to the extensive strain existing in the as-grown case. The slight split of the (0 0 ℓ) peaks between the PA film and the substrate indicates that significant strain relaxation must have occurred during annealing. In addition, as illustrated in Fig. 1(c), the X-ray scattering azimuthal scans of the PA film across the STO (2 2 2) and LSnMO (2 2 2) Bragg peaks, clearly show very narrow peak width and good alignment between the peak positions, indicating high-quality film crystallinity and the epitaxial relation between film and substrate after prolonged annealing.

To give a further account on the present results, we first note that in the PM state the resistivity for the AD and PA films (Fig. 2) differs drastically, by nearly two orders of magnitude. While this can be attributed to charge localization effects associated with lattice distortion [22,23], the absence of a temperature-induced T_{IM} in the AD film can be more subtle and complicated. De Teresa et al. [15] argued that it might be related to the absence of long-range FM order signified with a manifestation of spin-glass-like behavior at lower temperatures. This would imply that the large epitaxial strain originally existing in the AD film not only induces enormous charge localization effect but also hinders the formation of long-range FM ordering. If this argument is true, one expects to see the opposite for the PA films. At the first glance, it seems to explain the over 200% enhancement in magnetization and dramatic increase in T_{IM} rather consistently. However, since the $M(T)$ data were measured under an applied field of 0.1 T, the magnetizations of the samples are not yet saturated and cannot be used to estimate the saturated magnetic moment in the FM state. Instead we estimate the saturation magnetization of AD and PA films by using the results obtained from the magnetization vs. applied magnetic field (M–H) measurements. The estimated values for AD and PA films are, in the unit of Bohr magnetons (μ_B), $1.34\mu_B$ and $3.54\mu_B$, respectively. Though both values are still significantly less than the expected value of $4–5\mu_B$ for electron-doped manganites, it nevertheless shows

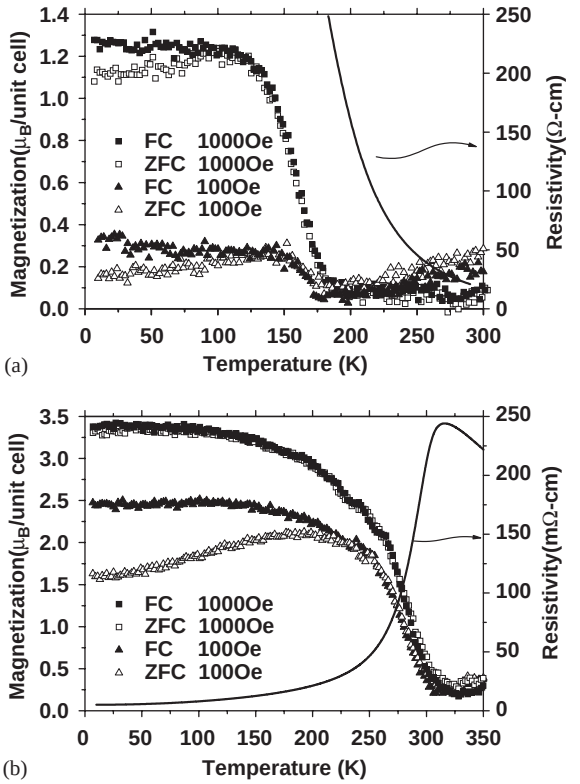

Fig. 2. The field-cooled and zero-field-cooled temperature-dependent magnetizations measured at 0.1 and 0.01 T for (a) the AD and (b) the PA films, respectively, showing that the typical spin-glass-like behavior occurs in both films. The zero-field temperature dependence of resistivity for both films is also displayed. Note the drastic difference exhibited.

an even pronounced enhancement in magnetization for PA films as compared to that implied in the $M(T)$ results taken at 0.1 T.

Despite of these seemingly consistencies with the strain-induced suppression of long-range magnetic ordering suggested by De Teresa et al. [15], we note, however, as shown in Fig. 2, significant spin-glass-like behavior, characterized by the pronounced irreversibility between the field-cooled (FC) and zero-field-cooled (ZFC) $M(T)$ curves, is evident for both cases. This implies that the insulator–metal transition and spin glass are not necessary mutually exclusive. Furthermore, Fig. 2 also reveals some features deviating from that reported for low-doping LSnMO [12]. That is, progressive suppression of spin-glass-like behavior with increasing Sn doping was observed and has been attributed to an increase of Mn^{4+} ions induced by La vacancies resulted from Sn doping. However, we suspect this scenario may not apply to our case. This is hinted firstly by the absence of impurity phase revealed by the XRD results and the stoichiometric composition of metallic ions observed. In addition, the 30% substitution of La by Sn would imply the existence of 90% Mn^{4+} ions [16], which will be well beyond the phase region exhibiting CMR effects in most manganites. Finally, we note that in our case ($x = 0.3$) the spin-glass transition not only emerges at a much higher temperature ($T_g \approx 250$ K) than that reported in Ref. [15] (75 K → 20 K for $x = 0.04 \rightarrow 0.18$) but also is very sensitive to the applied field. Apparently, the spin-glass-like behavior and CMR effect observed in the annealed LSnMO here, neither arise from Sn-doping-induced disorder [15] nor from the La-vacancy-induced divalent doping but are related to the strain relaxation in a more subtle manner. The other feature to be noted is the dramatic suppression of the low-temperature magnetization for the AD film when measured at 0.01 T. Since the basic ingredients for spin glass to occur are disorder and magnetic interaction randomness plus anisotropy and frustration [14], it would be interesting to conduct further experiments to delineate the underlying physics responsible for these observations.

Fig. 3 shows $\rho(T)$ as a function of applied field for the PA film. The resistivity was measured with the field applied parallel to the film surface. For the AD film, although there exists a typical PM–FM transition with $T_c \approx 175$ K, the $\rho(T)$ increases steeply with decreasing temperature (Fig. 2(a)) and has no sign of metallic transition for applied field up to 8 T. On the contrary, for the PA film, in addition to having nearly two orders of magnitude reduction in resistivity as compared to the AD film in PM state, it also displays typical CMR behavior with $T_{IM} = 314$ K at zero field. T_{IM} shifts to over 350 K at an applied field of 8 T. The maximum magnetoresistance (MR) ratio, defined as $\Delta\rho/\rho = (\rho(0) - \rho(H))/\rho(0)$ with $\rho(0)$ and $\rho(H)$ being the resistivity at zero field and that at field H, respectively, appears around 300 K

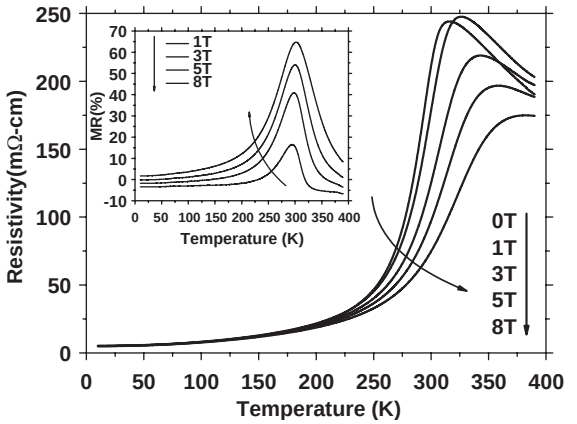

Fig. 3. $\rho(T)$ as a function of applied field for the PA LSnMO film. The inset illustrates the field dependence of MR ratio. Note that the maximum MR appears around the same temperature (~300 K) for all fields.

and reaches about 65% in a field of 8 T. Combining with the $M(T)$ results shown in Fig. 2 for both the AD and PA films, the results demonstrate that annealing not only changes the magneto-transport properties of the LSnMO films dramatically but also significantly enhances the magnetization by more than 200%. Guo et al. [11], by varying the film thickness in their $La_{0.9}Sn_{0.1}MnO_{3+\delta}$ films, have found similar enhancement in raising T_{IM} with increasing films thickness. However, there was no noticeable change in T_c and low-temperature magnetization with film-thickness variations, which led them to conclude that the enhancement of T_{IM} was due to strain relaxation instead of oxygen or La deficiency [5,6,16–20]. Similarly, Thomas et al. [21] have attributed the improved magneto-transport properties observed in their high-temperature (900 °C) annealed $La_{0.7}Ca_{0.3}MnO_3$ films to the massive stress relaxation and improved crystallinity accompanied with grain growth. However, they did not give how magnetization and T_c changed with annealing. From the present results (Fig. 1(a)–(c)), it appears that similar effects may have occurred in our case. The other possibility is that although post-annealing can improve the film crystallinity, it may also simultaneously yield La-deficient manganites [9]. In such a case, the material will become hole-doped and one expects to see enhanced manifestation of Mn^{4+}.

In order to check the effect of Sn doping on the valence states of Mn ions, XAS measurements were performed at the National Synchrotron Radiation Research Center of Taiwan. As is evident from the preliminary results shown in Fig. 4, the spectra of Mn-$L_{2,3}$ demonstrate that the present samples indeed display qualitative characteristics of Mn^{2+}/Mn^{3+} mixed-valence state, indicating that Sn doping does drive Mn^{3+} to Mn^{2+}. In particular, it is most discernible on the Mn-L_3 peak. As marked in Fig. 4, the peak positions of Mn^{2+}, Mn^{3+} and Mn^{4+} (obtained

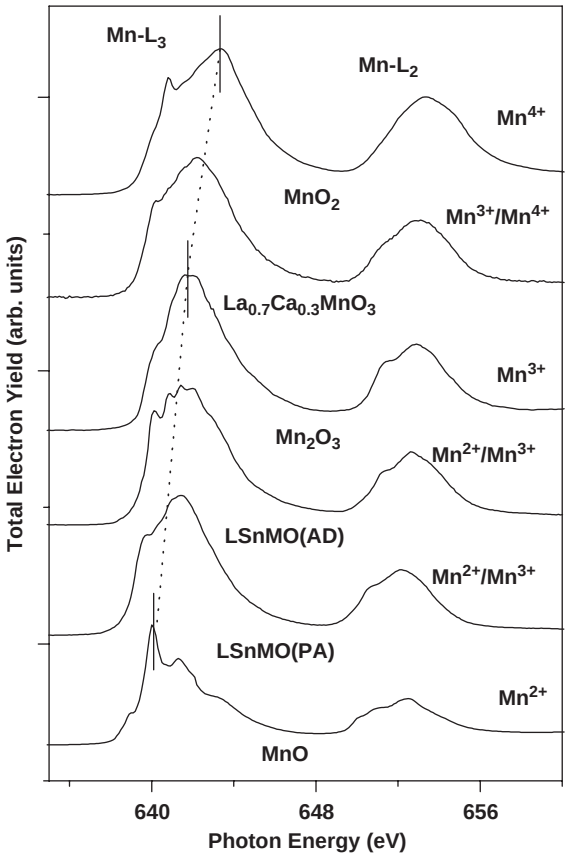

Fig. 4. The X-ray absorption spectra of Mn-$L_{2,3}$ for LSnMO film and various reference compounds. Note the evolution of the e_g-band peak as the valence of Mn ions changes from Mn^{4+}, Mn^{4+}/Mn^{3+}, Mn^{3+}, Mn^{3+}/Mn^{2+}, to Mn^{2+}, indicative of electron doping resulting from the tetravalent Sn-substitutions.

from the powder samples of MnO, Mn_2O_3, and MnO_2, respectively) are located at 640, 641.8, and 643.3 eV, respectively. On the contrary, the Mn-L_3 peak of LSnMO is situated between 640 and 642 eV and that of LCaMO is located somewhere around 642–644 eV. It is evident that both the AD and PA films are indeed of Mn^{2+}/Mn^{3+} mixing. We also find that there is noticeable difference between the detailed spectra of AD and PA films. Whether or not it is arising from the strain-induced effects is not clear at present. Detailed analyses along this line, including O-XAS, are certainly needed to give a more quantitative account on the exact nature of these Sn-doped manganites.

4. Conclusion

In summary, we have successfully prepared single-phase epitaxial $La_{0.7}Sn_{0.3}MnO_3$ films despite the tremendous challenges put forth by the large ionic size difference between La^{3+} and Sn^{4+}. The ex situ post-deposition annealing not only improves the structure of AD film and gives rise to epitaxial *c*-axis-oriented LSnMO films but also leads to above room temperature CMR effects. Both the AD and PA LSnMO films display significant features of spin glass that would need further studies for a complete understanding. Preliminary Mn L-edge XAS analysis shows features of Mn^{3+}/Mn^{2+} mixed-valence states, indicating that the tetravalent Sn ions indeed result in electron doping into e_g band of Mn.

Acknowledgements

We gratefully acknowledge Dr. J.M. Chen and Mr. J.M. Lee for the assistances in the XAS measurements. Work supported by the National Science Council of Taiwan, ROC, through Grant no. NSC93-2112-M009-016.

References

[1] Y. Tokura, N. Nagaosa, Science 288 (2000) 462 and references therein.
[2] E. Dagotto, Nanoscale Phase Separation and Colossal Magnetoresistance, Springer, Berlin, 2003 and references therein.
[3] V.L. Joseph Joly, P.A. Joy, S.K. Date, J. Magn. Magn. Mater. 247 (2002) 316.
[4] P. Mandal, S. Das, Phys. Rev. B 56 (1997) 15073.
[5] A. Gupta, T.R. McGuire, P.R. Duncombe, M. Rupp, J.Z. Sun, W.J. Gallagher, Gang Xiao, Appl. Phys. Lett. 67 (1995) 3494.
[6] S. Pingard, H. Vincent, J.P. Senateur, J. Pierre, A. Abrutis, J. Appl. Phys. 82 (1997) 4445.
[7] C. Mitra, P. Raychaudhuri, J. John, S.K. Dhar, A.K. Nigam, R. Pinto, J. Appl. Phys. 89 (2001) 524.
[8] W.J. Chang, C.C. Hsieh, J.Y. Juang, K.H. Wu, T.M. Uen, Y.S. Gou, C.H. Hsu, J.-Y. Lin, J. Appl. Phys. 96 (2004) 4357.
[9] T. Yanagida, T. Kanki, B. Vilquin, H. Tanaka, T. Kawai, Solid State Commun. 129 (2004) 785.
[10] J. Gao, S.Y. Dai, T.K. Li, Phys. Rev. B 67 (2003) 153403.
[11] X.X. Guo, S.Y. Dai, Y.L. Zhou, G.Z. Yang, Z.H. Chen, Appl. Phys. Lett. 75 (1999) 3378.
[12] X.X. Guo, Z.H. Chen, S.Y. Dai, Y.L. Zhou, R.W. Li, H.W. Zhang, B.G. Shen, H.S. Cheng, J. Appl. Phys. 88 (2000) 4758.
[13] A. Caneiro, L. Morales, F. Prado, D.G. Lamas, R.D. Sanchez, A. Serquis, Phys. Rev. B 62 (2000) 6825.
[14] J.A. Mydosh, Spin Glasses: An Experimental Introduction, Taylor & Francis, London, 1993.
[15] J.M. De Teresa, M.R. Ibarra, J. García, J. Blasco, C. Ritter, P.A. Algarabel, C. Marquina, A. del Moral, Phys. Rev. Lett. 76 (1996) 3392.
[16] S. de Brion, F. Ciorcas, G. Ghouteau, P. Lejay, P. Radelli, C. Chaillout, Phys. Rev. B 59 (1999) 1304.
[17] S.J. Kim, C.S. Kim, S.I. Park, B.W. Lee, J. Appl. Phys. 89 (2001) 7416.
[18] B.C. Hauback, H. fjellvag, N. Sakai, J. Solid State Chem. 124 (1996) 43.
[19] G.J. Chen, Y.H. Chang, H.W. Hsu, J. Magn. Magn. Mater. 219 (2000) 317.
[20] R. Suryanarayanan, J. Berthon, I. Zelenay, B. Martinez, X. Obradors, S. Uma, E. Gemelin, J. Appl. Phys. 83 (1998) 5264.
[21] K.A. Thomas, P.S.I.P.N. de Silva, L.F. Cohen, A. Hossain, M. Rajeswari, T. Venkateson, R. Hiskes, J.L. MacManus-Driscoll, J. Appl. Phys. 84 (1998) 3939.
[22] M.R. Ibarra, P.A. Algarabel, C. Marquina, J. Blasco, J. García, Phys. Rev. Lett. 75 (1995) 3541.
[23] P.G. Radaelli, D.E. Cox, M. Marezio, S.-W. Cheong, P.E. Schiffer, A.P. Ramirez, Phys. Rev. Lett. 73 (1995) 4488.